Infrared optical conductivity of the Nd-Ce-Cu-0 system

S. Lupi, P. Calvani, M. Capizzi, and P. Maselli
Dipartimento di Fisica, Università di Roma "La Sapienza," Piazzale Aldo Moro 2, I-00185 Roma, Italy

W. Sadowski and E. Walker
Section de Physique, Université de Genève, D.P.M.C., 24, quai Ernest-Ansermet, 1211 Genève 4, Switzerland
(Received 23 September 1991)

The reflectivity of seven $Nd_{2-x}Ce_xCuO_4$ single crystals has been measured at room temperature between 0.005 and 3 eV for $0 \leq x \leq 0.21$. At x=0, four transverse and longitudinal E_u phonon modes have been determined. Two bands have been also identified at 1.6 eV and at 2.8 eV, which lose their intensity with doping. Such intensity is transferred to the well-known Drude and midinfrared contributions, and to a band at $\sim$ 0.1 eV, which can be attributed to oxygen vacancies. At the insulator-to-metal transition, the Drude term abruptly increases, the 1.6-eV band vanishes. An overall strong similarity with the closing of the optical gap in highly doped semiconductors, is found. The reflectivity of a reduced sample with x =0.07 suggests that the midinfrared band may not originate from oxygen vacancy states. Present results are compared with predictions of different theoretical models.

I. INTRODUCTION

It is well established[1] that the normal-state optical response in the range from 0 to $\approx$3 eV, for all families of high-T_c superconductors (HTCS), can be described in terms of a Drude-Lorentz complex dielectric function, whose general formula is

$$\tilde{\epsilon}(\omega) = \epsilon_\infty - \frac{\omega_p^2}{\omega^2 + i\omega\Gamma_D} + \sum_j \frac{S_j^2}{(\omega_j^2 - \omega^2) - i\omega\Gamma_j} + \frac{S_{\mathrm{MIR}}^2}{(\omega_{\mathrm{MIR}}^2 - \omega^2) - i\omega\Gamma_{\mathrm{MIR}}} + \sum_i \frac{S_{\mathrm{CT}i}^2}{(\omega_{\mathrm{CT}i}^2 - \omega^2) - i\omega\Gamma_{\mathrm{CT}i}} . \quad (1)$$

The contributions to $\tilde{\epsilon}(\omega)$ in Eq. (1) are given by a Drude absorption (D) with plasma frequency ω_p and width Γ_D, phonons (ph) of frequencies ω_j, linewidths Γ_j, and strengths S_j, a midinfrared (MIR) band at ω_{MIR}, a charge-transfer (CT) band modeled by oscillators at $\omega_{\mathrm{CT}i}$, and finally ϵ_∞, which includes all higher-energy transitions. The relative weight of these contributions is related to the number of carriers in the Cu-O plane, which in turn depends upon the concentration of dopant x and/or the amount of oxygen nonstoichiometry y in the cuprate formula. For undoped stoichiometric insulators ($x = y = 0$), both the Drude and the midinfrared terms in Eq. (1) vanish. On the other hand, in good metallic samples some charge transfer contributions may vanish, while phonons are screened by free carriers (nonetheless, far-infrared features in a superconducting Y-Ba-Cu-O film have been attributed to phonons[2] strongly coupled to holes).

The MIR contribution to $\tilde{\epsilon}(\omega)$ is centered at energies which may vary from 0.1 to 0.7 eV, depending upon the high-T_c superconductor family and, as in $Bi_2Sr_2Ca_nCu_{n+1}O_{2n+6}$, on the crystal phase n.[3] In $Nd_{2-x}Ce_xCuO_4$, this contribution has been observed by several authors[4–7] at about 0.5 eV.[6] In spite of its reproducibility, the MIR band has been explained in the literature by entirely different models, like Holstein processes,[8] Holstein-like processes involving magnons,[9] a marginal Fermi liquid,[10] or the effect of doping on charge-transfer transitions.[11]

Bands attributed to charge-transfer transitions between O 2p and Cu 3d states have been observed in the insulating phases of Y-Ba-Cu-O, Bi-Sr-Ca-Y-Cu-O, La-Sr-Cu-O, and M-Ce-Cu-O (M=Nd, Pr, Sm, Eu, Gd). In the undoped insulator, the CT band can be adequately reproduced by the superposition of two oscillators, which are centered at 2.0 and 3.0 eV in La-Sr-Cu-O,[12] at 1.5 and 2.1 eV in Nd-Ce-Cu-O.[13] In Nd_2CuO_4, the former oscillator is shifted toward lower frequencies when Nd is replaced by Pr, toward higher frequencies when it is replaced by Sm, Eu, or Gd.[14] A connection has been experimentally established between the CT band and the midinfrared contribution: spectral weight is transferred from the CT band to the MIR band (and to the Drude term), as holes or electrons are injected into the Cu-O plane by doping. This effect has been observed in La-Sr-Cu-O,[12] in Pr-Ce-Cu-O,[15] and also in $Nd_{2-x}Ce_xCuO_4$ (where two samples, with x=0 and x=0.2, were compared).[16]

The above picture successfully describes the most relevant features of the optical properties of HTCS, both in the insulating phase and in the metallic one. However, deviations of these materials from ideal conditions, like lack of stoichiometry or homogeneity, or peculiar point defects, may give rise to a more complex scenario. In particular, several structures have been observed in the infrared absorption spectra of insulating $SrTiO_3$,[17] a perovskite-type oxide which becomes superconducting

when doped by Nb (Ref. 18) or oxygen vacancies.[19] These structures have not been yet identified, although some attempts to explain them in terms of impurity levels or localized defects with a strong polar interaction, have been made.[17] Moreover, three low-energy bands have been recently observed in $Nd_2CuO_{4-0.03}$ and attributed to electronic states induced by oxygen nonstoichiometry.[20,21] Finally, a nonhomogeneity in the Ce concentration x, leading to the formation of a thin metallic film on the top of an insulating bulk, has been invoked to explain a deep in the far-infrared (FIR) reflectivity spectra of metallic $Nd_{2-x}Ce_xCuO_4$ with $x = 0.15$.[6] In the following study of the normal state optical properties of the electron-doped material $Nd_{2-x}Ce_xCuO_{4-y}$,[22] we will therefore add to Eq. (1) a term

$$\sum_k \frac{S_{dk}^2}{(\omega_{dk}^2 - \omega^2) - i\omega\Gamma_{dk}} \tag{2}$$

to account for the possible presence of point defects in our samples.

The aim of this paper is to study in detail how the various contributions to the optical conductivity discussed above evolve as Ce doping progressively injects electrons into the Cu-O planes. Moreover, it is intended to investigate the possible role of point defects, like oxygen vacancies, in the optical properties of HTCS. It will be evidentiated that the optical gap undergoes a transformation very like that reported for highly doped semiconductors. Finally, our results will be compared with those of similar investigations on hole-doped $La_{2-x}Sr_xCuO_{4-y}$,[12] and electron-doped $Pr_{2-x}Ce_xCuO_4$,[15] as well as with the results of theoretical studies.

II. EXPERIMENTAL DETAILS

The reflectivity $R(\omega)$ of $Nd_{2-x}Ce_xCuO_{4-y}$ single crystals, with y=0 and x=0.0, 0.04, 0.122, 0.15, 0.17, and 0.21, has been measured. Such a range of values covers the insulating and the metallic phases of Nd-Ce-Cu-O up to the limit of Ce solubility (x=0.21). An insulator-to-metal transition at $x = x_{MIT} = 0.125$ divides the two phases.[23] A $y > 0$ sample, with x=0.07, has been also investigated. None of the samples here examined was superconducting. Indeed, superconductivity in Nd-Ce-Cu-O is observed for $0.13 < x < 0.18$, once a reduction procedure has produced a significant number of oxygen vacancies (i.e., $y > 0$).

Sample preparation and characterization, as well as the infrared experimental setup, have been described in detail in previous papers[6,23] and are outlined here. Single crystals of $Nd_{2-x}Ce_xCuO_4$ were grown from a mixture of Nd_2O_3, CeO_2, and Cu_2O, which was rapidly heated from room temperature to 1250 °C, soaked for 30–60 min, then slowly cooled to 1050 °C at a rate of 3 °C/h, and finally quenched outside the furnace. The single crystals were separated mechanically from the crucible and then analyzed by scanning electron microscope (SEM) and energy dispersive x-ray analysis (EDAX). Within the instrument accuracy, the distribution of Ce and Nd in the (001) surface and along the [001] direction is homogeneous. The final concentration of Ce resulted in depending very weakly on the nominal composition, and the maximum observed value was x=0.21. The values reported for x in this paper were obtained by performing a chemical microanalysis at 4 to 7 points of the crystal surface, and then calculating the average Ce concentration.

The reflectance $R(\omega)$ was measured from 50 to 25 000 cm^{-1} by a rapid scanning interferometer. The light beam, 0.5 mm in diameter, was incident under vacuum on the sample at an angle of 8°, so that the electric field was predominantly in the Cu-O plane. The reference was a Au-film evaporated on a sapphire window in the infrared, a polished platinum foil in the visible and near UV. The present work is restricted to data taken at room temperature. Preliminary measurements at 20 K on a sample with $x = 0.17$ do not show any major change in $R(\omega)$, for $\omega > 500$ cm^{-1}, thus confirming previous findings.[5]

III. RESULTS AND DISCUSSION

The infrared reflectivity spectra of "as-grown" $Nd_{2-x}Ce_xCuO_4$ samples are given by dots in Fig. 1, for various Ce concentrations x. The far-infrared spectra of the insulator Nd_2CuO_4 and of the metallic $Nd_{1.85}Ce_{0.15}CuO_4$ samples are shown in the inset. Both of them are consistent with previous observations on single crystals.[16,24,25] The solid lines in Fig.1 have been obtained by fitting $R(\omega)$ to the usual expression for reflectivity at normal incidence

$$R(\omega) = \left|(1 - \sqrt{\tilde{\epsilon}})/(1 + \sqrt{\tilde{\epsilon}})\right|^2 , \tag{3}$$

where $\tilde{\epsilon}(\omega)$ is given by Eq. (1).

The insulator Nd_2CuO_4 is described by Eq. (1), with $\omega_p = S_{MIR} = 0$. The resulting imaginary part of the dielectric constant, ϵ_2, is shown for the far-infrared region in Fig. 2(a). Four E_u transverse optical (TO) phonon modes are infrared active in the Cu-O plane of the T′

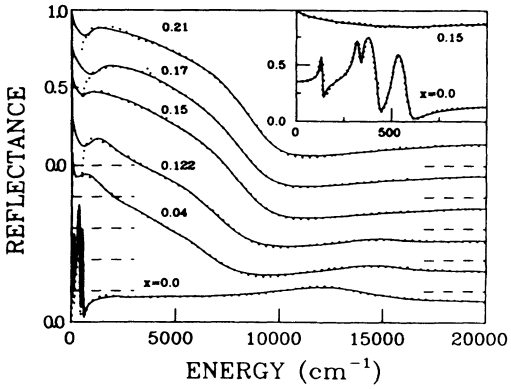

FIG. 1. The reflectance $R(\omega)$ of "as-grown" $Nd_{2-x}Ce_xCuO_4$ samples is plotted for various Ce concentrations x. The far-infrared reflectivities of an insulating (x=0) and of a metallic (x=0.15) single crystal, are shown in the inset. Experimental data are given by dots, best fits by solid lines.

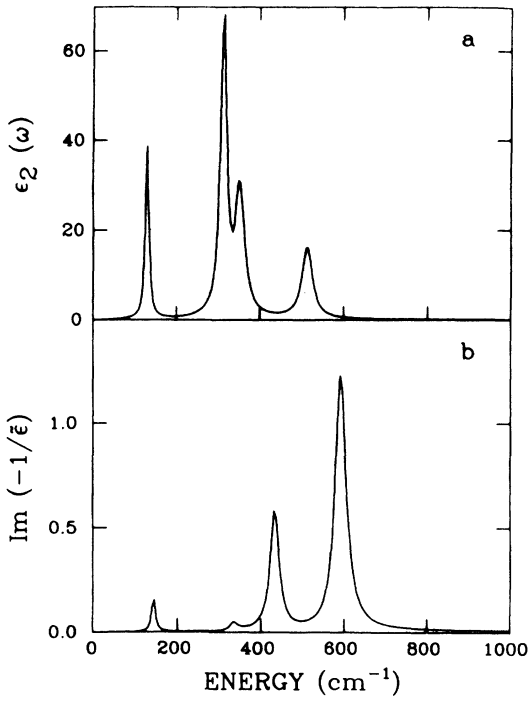

FIG. 2. Far-infrared ϵ_2 (a) and Im$[-1/\tilde{\epsilon}(\omega)]$ (b) for the insulator Nd_2CuO_4, obtained as explained in the text. Peaks in (a) correspond to TO phonons, in (b) to LO phonons.

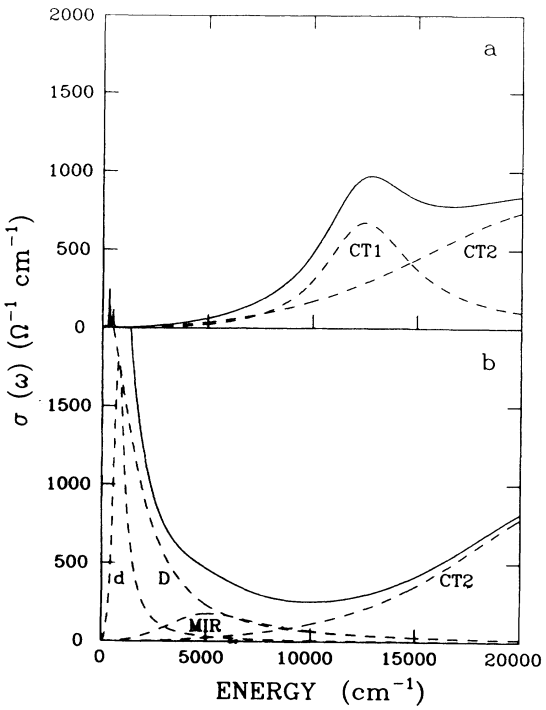

FIG. 3. The real part of the optical conductivity $\sigma(\omega)$, solid line, is plotted for the x=0 (a) and x=0.15 (b) samples, together with individual contributions $\sigma^{\alpha}(\omega)$, dashed lines.

structure.[24] All of them are well resolved in Fig. 2(a). The function Im$[-1/\tilde{\epsilon}(\omega)]$, plotted in Fig. 2(b), is peaked at the longitudinal optical (LO) phonon frequencies, ω_{jL}, under the assumption that the phonon lines are narrow,[26] as realized in the present case. All the parameters for the TO and LO phonons of Nd_2CuO_4 are reported in Table I. Therein, they are compared with those obtained by other authors who used Kramers-Krönig relations in the analysis of R(ω),[16,24,25] instead of the present fit to a Drude-Lorentz model. The close agreement among these results provides good evidence of the equivalence among these different procedures.[27] In a previous experiment,[6] a fifth oscillator at 190 cm^{-1} was detected in a Nd_2CuO_4 sample and was interpreted in terms of some distortion of the tetragonal T′ structure. Heyen *et al.*[24] attributed a corresponding additional peak, at 165 cm^{-1} in $R(\omega)$, to some magnetic excitation. Present data on new single crystals do not confirm such findings, as it is apparent in Fig. 2(a). The parameters of the oscillators CT1 and CT2, which describe the charge transfer band in the insulator, are also listed in Table I. It has to be mentioned that a large uncertainty affects the energy of CT2, whose peak energy falls at $\simeq$ 22 500 cm^{-1} (2.8 eV), close to the upper limit of the measured energy range.

The infrared reflectivity of $Nd_{2-x}Ce_xCuO_4$ changes dramatically as Nd is increasingly replaced by Ce and carriers are injected into the Cu-O planes, as shown in Fig. 1 and previously reported.[4–7,16] Although a best fit to $R(\omega)$ has been obtained in terms of $\tilde{\epsilon}$, the different spectral contributions to R(ω) can be discussed more easily in terms of the real part of the optical conductivity

$$\sigma(\omega) = (\omega/4\pi)\epsilon_2 = \sum_{\alpha} \sigma^{\alpha}(\omega) \ , \qquad (4)$$

where α = ph, D, d, MIR, CT1, CT2.

The individual contributions $\sigma^{\alpha}(\omega)$, as well as the total $\sigma(\omega)$, are reported in Fig. 3 for the single crystals with x=0 and x=0.15. In addition to the four E_u phonon peaks, Fig. 3(a) displays the CT1 and CT2 bands, namely, the two charge transfer contributions at much higher frequencies already reported in Table I for the x=0 sample. For the metallic x=0.15 sample, instead, Fig. 3(b) shows intense D and d contributions as well as the loss of the CT1 band at $\simeq$ 13 000 cm^{-1} (1.6 eV). This suggests that the addition of Ce donors results in a transfer of spectral weight among the different terms of Eq. (4). This can be followed better in Fig. 4, where the differences between total $\sigma(\omega)$'s corresponding to different x's are plotted. The difference $[\sigma(\omega)]_{0.04}-[\sigma(\omega)]_{0.0}$ [see Fig. 4(a)] clearly shows that at low doping the MIR band is built up by transferring spectral weight from both the CT1 and CT2 bands to lower energy. However, it is quite surprising to see the appearance of a weak and narrow Drude-like term in the x=0.04 sample, an insulator from transport measurements. A similar term has been also reported for insulating $La_{2-x}Sr_xCuO_{4-y}$.[12] A further increase of doping exhausts the CT1 band, as shown in Fig. 4(b) by the difference $[\sigma(\omega)]_{0.15}-[\sigma(\omega)]_{0.04}$, thus turning the crystal into a metal (x_{MIT} = 0.125) with

TABLE I. Oscillator frequencies, linewidths, and strengths, in cm^{-1}, entering $\tilde{\epsilon}(\omega)$ as obtained from $R(\omega)$ in Nd_2CuO_4 single crystals at room temperature. Data from Crawford *et al.* have been taken at 10 K. Symbols are referred to Eq. (1).

Mode	Parameter	This work	Zhang *et al.* (Ref. 16)	Heyen *et al.* (Ref. 24)	Crawford *et al.* (Ref. 25)
E_{u1}	ω_1	130	121	132	129
	Γ_1	10	16		9
	S_1	200			250
	ω_{1L}	141	138	139	140
E_{u2}	ω_2	314	301	304	300
	Γ_2	13	8		11
	S_2	560			920
	ω_{2L}	336	335	341	342
E_{u3}	ω_3	352	347	353	350
	Γ_3	28	12		12
	S_3	550			360
	ω_{3L}	430	426	432	437
E_{u4}	ω_4	514	507	512	509
	Γ_4	29	44		17
	S_4	490			520
	ω_{4L}	598	608	593	595
CT1	ω_{CT1}	12500			
	Γ_{CT1}	5200			
	S_{CT1}	14400			
CT2	ω_{CT2}	22500			
	Γ_{CT2}	21700			
	S_{CT2}	31800			
	ϵ_∞	1.8	7		6.8

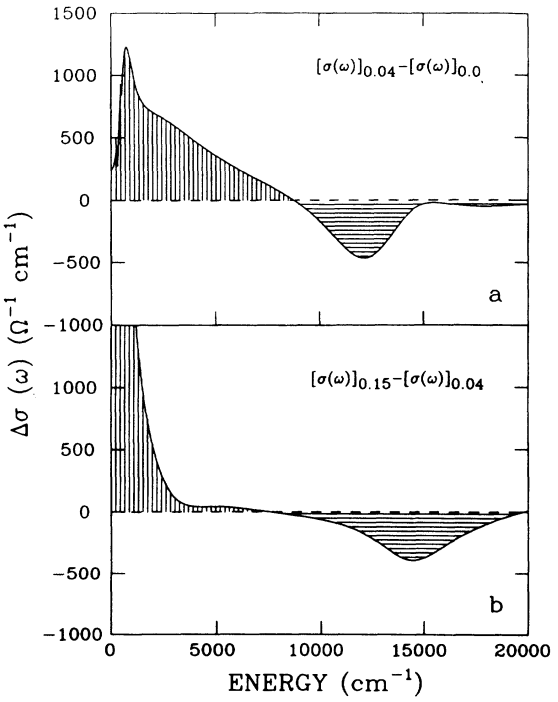

FIG. 4. The differences $[\sigma(\omega)]_{0.04} - [\sigma(\omega)]_{0.0}$ (a) and $[\sigma(\omega)]_{0.15} - [\sigma(\omega)]_{0.04}$ (b) are plotted vs energy.

a fully developed Drude term. Only minor changes are instead observed in this same domain of x in the midinfrared region of the spectrum and in the CT2 band.

We shall now analyze in detail how individual contributions to $\sigma(\omega)$ change with x. First of all, notice that all those contributions have well-identified energies which undergo minor changes over the whole range of Ce solubility, as shown in Fig. 5. Only ω_{MIR} seems to increase smoothly with x (with a possible small shift at the insulator-to-metal transition).

The effect of doping is usually described in terms of the effective number of carriers

$$n_{eff} = \frac{2m^*V}{\pi e^2}\int_0^\infty \sigma(\omega)\,d\omega\ , \tag{5}$$

where, in a first approximation, the effective mass m^* is assumed to be the free-electron mass m_0 and V is the volume of the cell which contains one formula unit (188×10^{-24} cm^3 in the present case). Because $\sigma(\omega)$ is usually obtained by Kramers-Krönig transformations of $R(\omega)$ over a finite-energy range,

$$n_{eff}(\omega) = \frac{2m^*V}{\pi e^2}\int_0^\omega \sigma(\omega')\,d\omega' \tag{6}$$

is normally reported. The procedure used here of fitting the reflectance data to a Drude-Lorentz model allows us

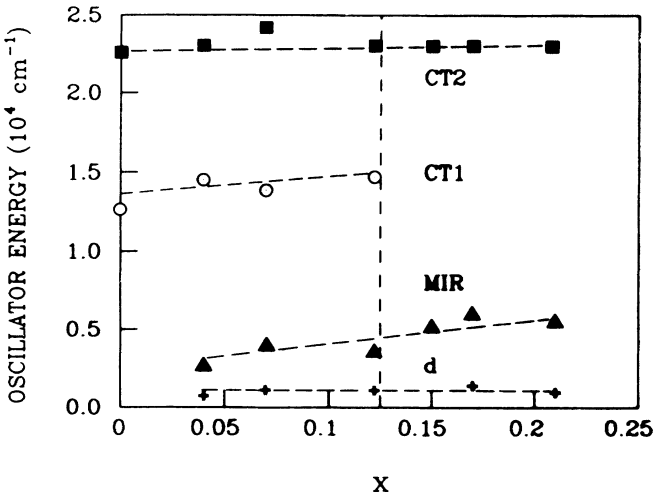

FIG. 5. Energies of d, MIR, CT1, and CT2 oscillators in Eq. (1), are plotted as a function of x for $Nd_{2-x}Ce_xCuO_{4-y}$. All single crystals are "as-grown" ($y \simeq 0$) but the one with x=0.07, which has $y > 0$. Dashed lines are guides to the eye only.

instead to get an estimate of $\sigma(\omega) = \sum_\alpha \sigma^\alpha(\omega)$ from zero energy to infinity, *limitedly* to the contributions α's here considered, and therefore to get

$$n_{\text{eff}}^{\text{total}} = \sum_\alpha n_{\text{eff}}^\alpha = \sum_\alpha \frac{2m^* V}{\pi e^2} \int_0^\infty \sigma^\alpha(\omega)\, d\omega \ , \qquad (7)$$

where α = ph, D, d, MIR, CT1, CT2.

We now discuss the behavior with x of the strengths of the different processes contributing to the optical conductivity and described by the effective charges n_{eff}^α, which are reported in Fig. 6. First of all, $n_{\text{eff}}^{\text{total}}$ increases linearly with x starting from a value $\simeq 2.5$ at x=0. Over the range of concentrations here considered, $\Delta x = 0.21$, n_{eff} changes by $\Delta n_{\text{eff}} = 0.1 \pm 0.1$. Assuming that, as found in $La_{2-x}Sr_xCuO_{4-y}$,[12] the Ce doping is entirely accounted for by the additional effective charge of the oscillators at energy lower than 3 eV, this would imply that the average effective mass of these oscillators is of the order of two.

As soon as some degree of disorder is introduced into the system (x=0.04), the MIR band, which is absent in the x=0 sample, reaches its maximum strength. At the same time, small D- and d-band contributions are required in order to get a good fit to the data. For higher Ce concentrations (x=0.122), the MIR band *substantially decreases* in favor of the d band, which therefore increases. Such opposite behavior extends to higher Ce concentrations, resulting into a sum $n_{\text{eff}}^{\text{MIR}} + n_{\text{eff}}^{\text{d}}$ roughly constant over all x's. The Drude term shows a major change ($\Delta n_{\text{eff}}^D \simeq 0.3$) at the insulator-to-metal transition x_{MIT}, followed by a linear increase for $x > x_{\text{MIT}}$. The low-energy effective charge ($D + d$ + MIR) follows the behavior of the D term. This excess charge is provided by the Ce doping as well as by a weakening of the high-energy bands CT1 and CT2, as shown in Fig. 6(b). The two oscillators accounting for the charge transfer band, however, have a quite different behavior: $n_{\text{eff}}^{\text{CT1}}$ decreases for increasing Ce doping until it collapses to zero for $x > 0.122$, as verified by repeated tests of our fitting procedure; $n_{\text{eff}}^{\text{CT2}}$ decreases at low doping, it saturates at high doping. The assignment of the CT1 band to a Cu-O charge transfer is consistent with the abrupt decrease of its strength as soon as screening effects become important (i.e., for $x \geq x_{\text{MIT}}$), while the assignment of the CT2 band to the same process is questionable. The continuous transfer of effective charge from higher to lower energies in the insulating phase (CT1+CT2$\rightarrow$ MIR + d and MIR $\rightarrow$ D + d), as well as the sudden change of the Drude contribution at $x = x_{\text{MIT}}$, reminds one of the closing of an optical gap observed in highly doped semiconductors like Si:P.[28] Further measurements, in particular at x <0.04 and $x \sim x_{\text{MIT}}$, are needed to clarify the role, if any, of the insulator-to-metal transition in these

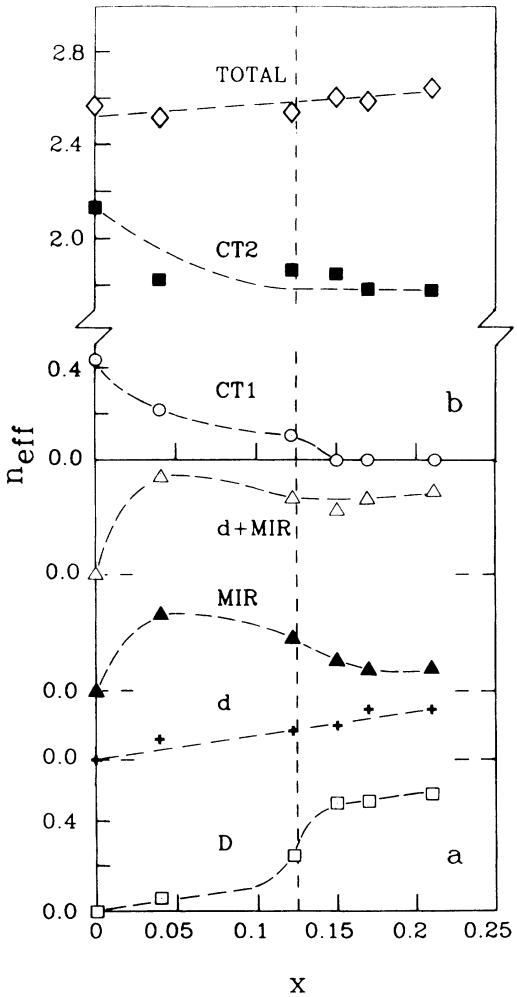

FIG. 6. The effective charges n_{eff}^α entering Eq. (7), and their combinations, are plotted as a function of x for $Nd_{2-x}Ce_xCuO_4$ single crystals with $y \simeq 0$. The lines are a guide to the eye only. The insulator-to-metal transition at x_{MIT}=0.125 is marked in the figure.

processes as well as to identify the nature of the low-energy bands. Nevertheless, some speculations can be made on the ground of available results. Oxygen vacancies are intrinsic point defects in perovskite-type oxides, which are responsible for the superconductivity reported in $YBa_2Cu_3O_{7-y}$, $Bi_2Sr_2Ca_nCu_{n+1}O_{2n+6}$, and $SrTiO_3$. These defects give rise to structures at 0.16, 0.35, and 0.76 eV in Nd_2CuO_{4-y} with y=0.03.[20] The structures observed[17] at 0.163, 0.364, and $\sim$ 0.4 eV in $SrTiO_3$ could likely be due to similar deviations from stoichiometry. Finally, a broad oscillator, centered at $\omega \sim 0.13$ eV, has been reported in $Bi_2Sr_2Ca_nCu_{2n+1}O_{2n+6}$.[3,29] The introduction of low-frequency oscillators—observed also in reduced samples, not reported here—is therefore required in a number of different materials.[30]

It is then tempting to correlate the MIR and d bands observed in the present work with oxygen vacancies, whose concentration may easily exceed the thermodynamic value. As far as the d band is concerned, it is related to contributions peaked at 0.10±0.05 eV, whose strength increases smoothly with x. Oxygen vacancy concentration increases with Sr doping in $La_{2-x}Sr_xCuO_{4-y}$[12] and it is expected to do the same with Ce doping in $Nd_{2-x}Ce_xCuO_{4-y}$. In order to verify if the MIR band observed here at $\omega \leq 0.7$ eV may also correlate with oxygen vacancies—in particular with the second strongest band observed at $\omega = 0.76$ eV (Ref. 20)—an x=0.07 reduced crystal has been carefully studied. This sample has been obtained by a 10-h exposure to a 1-bar nitrogen atmosphere at 900 °C. The reflectivity and the conductivity resulting from the fitting procedure of this $Nd_{1.93}Ce_{0.07}CuO_{4-y}$ sample ($y > 0$) are shown in Figs. 7(a) and 7(b), respectively. In addition to the FIR phonon peaks and to the two high-energy charge transfer bands, three contributions instead of the d and MIR ones have to be introduced in order to account for the midinfrared region ($\omega_{d1} = 0.10$ eV, $\Gamma_{d1} = 0.18$ eV, $n_{\rm eff}^{d1} = 0.05$; $\omega_{d2} = 0.49$ eV, $\Gamma_{d2} = 0.61$ eV, $n_{\rm eff}^{d2} = 0.10$; $\omega_{d3} = 0.72$ eV, $\Gamma_{d3} = 0.57$ eV, $n_{\rm eff}^{d3} = 0.11$). As far as bands $d1$ and $d3$ are concerned, they are in good agreement with those attributed to oxygen vacancies for a reduced ($y > 0$) Nd_2CuO_{4-y} sample.[20] On the other hand the band $d2$ can be well identified with the MIR band observed in the "as-grown" y=0 samples. The simultaneous observation of $d1$ and $d3$ oxygen bands and of the $d2 \equiv$ MIR band suggests that the MIR band may not be related to oxygen vacancies.

A feature which singles out Nd_2CuO_{4-y} among all other high-T_c superconductors is that both doping and reduction are needed to get superconductivity. A detailed comparison of the present data with the optical conductivity of superconducting samples may provide a novel approach to the understanding of the onset of superconductivity in oxides. No systematic collection of optical data is presently available in the superconducting region. An analysis in terms of a Drude-Lorentz model has been performed for an x =0.15 single crystal with T_c = 18 K.[6] This sample showed an appreciable decrease of $R(\omega)$, with an ensuing reduction of $n_{\rm eff}^D$, with respect to an as-grown sample with the same x. This effect, which cannot be straightforwardly explained for an n-type superconductor, will be the object of a separate investigation.

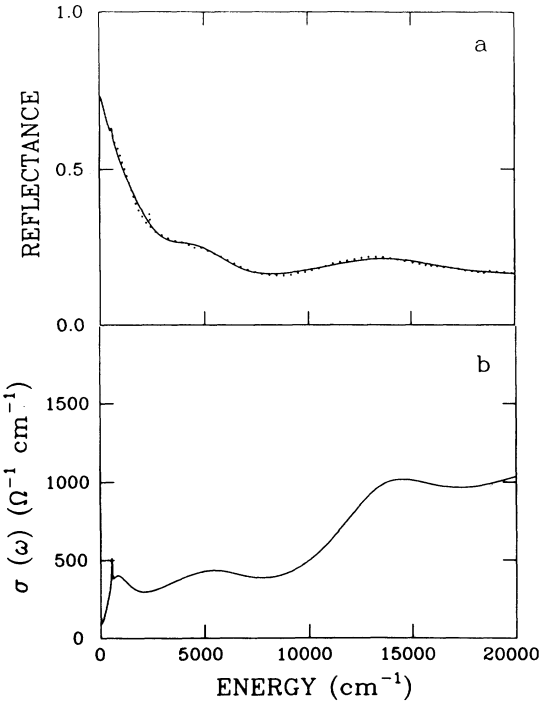

FIG. 7. $R(\omega)$ (a) and $\sigma(\omega)$ (b) for the $Nd_{2-x}Ce_xCuO_{4-y}$ single crystal with x=0.07 and $y > 0$.

The results of the present work will be now compared with those collected in other oxide superconductors, as well as with theoretical results. Although an analysis in terms of the evolution of each $n_{\rm eff}^{\alpha}$ has not yet been done, the reflectivity measured in $La_{2-x}Sr_xCuO_4$[12] and $Pr_{2-x}Ce_xCuO_{4-y}$[15] changes with doping x very like that measured in $Nd_{2-x}Ce_xCuO_{4-y}$ does.

In $La_{2-x}Sr_xCuO_4$,[12] two CT bands have been observed, with CT2 (at 3 eV) much broader than CT1 (at 2 eV). Their line shapes and their oscillator energy ratio $\omega_{CT2}/\omega_{CT1}$ reproduce those observed here. A continuous transfer of strength seems to take place from the CT1 band to a MIR band at 0.8 eV, as well as to lower energies, for increasing Sr doping. This transfer is already appreciable for x=0.02 and keeps going up to $x_{\rm MIT} \simeq 0.06$, where the CT1 contribution practically vanishes. At the same time, the CT2 band, attributed to transitions from O 2p to La 5d/4f or Cu 4s/4p levels, does not visibly change for $0.0 \leq x \leq 0.25$, while it decreases at higher x where the material ceases to be superconducting. The Drude term shows up already in the insulating phase, where it increases linearly with x, with $n_{\rm eff}^D << x$. Similar qualitative considerations should hold for $Pr_{2-x}Ce_xCuO_{4-y}$,[15] where the behavior of the reflectivity raw data well reproduces that observed for the present Nd-based compound.

We will now use present results to verify some predictions of different theoretical models of HTCS.

A variety of Fermi-liquid approaches have found that $\omega_p^2 \propto x$.[31–35] This behavior is well followed by the present $n_{\rm eff}$ ($\propto \omega_p^2$), which moreover shows an abrupt change at $x_{\rm MIT}$, not accounted for by the theory. One of these models[35] also predicts a linear increase with x for the spectral weight of the MIR band. From our results, instead, $n_{\rm eff}^{\rm MIR}$ *decreases* with x after having reached its maximum at the lowest measured Ce concentration, while a roughly constant behavior with x is obtained if the contribution of the d term is included in the MIR one (i.e., for $n_{\rm eff}^{\rm MIR} + n_{\rm eff}^{d}$).

For what concerns the t-J models,[36,37] developed to explain the h-doped HTCS, they predict, among other results, a MIR band whose energy shifts toward lower energies as doping increases. This behavior is opposite to that observed in the present work. The same is true even if the contribution of the d band is included in the MIR band. One cannot exclude that this discrepancy may be due to the injection of electrons, instead of holes, in the Cu-O planes.

Finally, the present results on $Nd_{2-x}Ce_xCuO_4$, as well as the above findings on $La_{2-x}Sr_xCuO_4$,[12] are consistent with recent theoretical estimates of Tohyama and Maekawa.[38] They evaluated $\sigma(\omega)$ and $n_{\rm eff}$ for undoped, 25% h-doped, and 25% e-doped Cu-O planes in a Cu_4O_{13} cluster. In addition to minor contributions, the undoped Cu-O plane is reported to exhibit two strong CT bands at 1.4 and 2.1–2.8 eV, in very good agreement with our results for Nd_2CuO_4. Moreover, strong electron doping causes the CT1 band to disappear and an intense Drude term to appear, while the CT2 band survives even if it partially loses its spectral weight. These predictions are consistent with the experimental results reported in Fig. 6.

IV. CONCLUSIONS

Reflectivity measurements have been performed at room temperature in as-grown $Nd_{2-x}Ce_xCuO_4$ single crystals for x's spanning from the insulating to the metallic phase, up to the limit of Ce solubility (x=0.21). Their strong resemblance with measurements in $La_{2-x}Sr_xCuO_4$[12] (and in $Pr_{2-x}Ce_xCuO_{4-y}$)[15] has first shown in detail that the behavior with doping of the optical properties of h-doped and e-doped materials is the same. This agrees well with recent theoretical estimates of the conductivity in these superconducting oxides.[38] Some discrepancies between present results and predictions based on the marginal Fermi liquid and the t-J models, have been pointed out. The total effective charge $n_{\rm eff}^{\rm total}$ shows a linear dependence on x, which is consistent with a value of two for the effective mass averaged over the energy range 0–3 eV. The modeling of the dielectric constant in terms of a Drude term plus Lorentz oscillators has also allowed to evaluate the effective charges for the individual contributions to the optical response, as well as their dependence on x. In addition to the well-known Drude and midinfrared bands, a novel band has been detected at low energy ($\sim$ 0.1 eV). This band has been attributed to states induced by oxygen vacancies on the ground of a comparison with an x=0.07 reduced sample—confirmed by preliminary results on other reduced samples—as well as with recent results.[20,21] On the same ground, it seems likely that energy levels due to oxygen vacancies are not involved in the transition responsible for the MIR band, whose origin is therefore still unclear. The Drude and the lower energy charge transfer bands are strongly affected by the insulator-to-metal transition, the former band sharply increasing, the latter instead vanishing at the transition. The overall behavior of the raw reflectivities and of effective charges as a function of x is very similar to that observed in highly doped semiconductors. An extension of this study to $x < 0.04$, as well as a detailed investigation for x's around the insulator-to-metal transition, is needed to establish a more firm correlation between the optical properties here reported and specific point defect states, as opposed to a purely intrinsic behavior.

ACKNOWLEDGMENTS

This work supported by Progetto SATT of Consorzio INFM and by Progetto Finalizzato Superconduttività of Consiglio Nazionale delle Ricerche.

[1] T. Timusk and D.B. Tanner, in *Infrared Properties of High T_c Superconductors*, in *Physical Properties of High Temperature Superconductors*, edited by D.M. Ginsberg (World Scientific, Singapore, 1989), pp. 339-407, and references therein.

[2] T. Timusk, C. D. Porter, and D. B. Tanner, Phys. Rev. Lett. **66**, 663 (1991).

[3] P. Calvani, M. Capizzi, S. Lupi, P. Maselli, D. Peschiaroli, and H. Katayama-Yoshida, Solid State Commun. **74**, 1333 (1990).

[4] K Hirochi, S. Hayashi, H. Adachi, T. Mitsuyu, T. Hirao, K. Setsune, and K. Wasa, Physica C **160**, 273 (1989).

[5] Y. Watanabe, Z. Z. Wang, S. A. Lyon, N. P. Ong, D. C. Tsui, J. M. Tarascon, and E. Wang, Solid State Commun. **74**, 757 (1990).

[6] P. Calvani, M. Capizzi, S. Lupi, P. Maselli, M. Virgilio, A. Fabrizi, M. Pompa, W. Sadowski, and E. Walker, J. Less-Common Met. **164&165**, 776 (1990).

[7] S. Uchida and H. Takagi, Physica C **162-164**, 1677 (1989).

[8] S. L. Cooper, G. A. Thomas, J. Orenstein, D. H. Rapkine, M. Capizzi, T. Timusk, A. J. Millis, L. F. Schneemeyer, and J. V. Waszczak, Phys. Rev. B **40**, 11 358 (1989).

[9] C. X. Chen and H. B. Schüttler, Phys. Rev. B **43**, 3771 (1991).

[10] C. M. Varma, P. B. Littlewood, S. Schmitt-Rink, E. Abrahams, and A. E. Rukenstein, Phys. Rev. Lett. **63**, 1996 (1989).

[11] I. Terasaki, T. Nakahashi, S. Takebayashi, A. Maeda, and K. Uchinokura, Physica C **165**, 152 (1990).

[12] S. Uchida, T. Ido, H. Takagi, T. Arima, Y. Tokura, and

S.Tajima, Phys. Rev. B **43**, 7942 (1991).
[13]S. Uchida, Mod. Phys. Lett. B **4**, 513 (1990).
[14]S. L. Cooper, G. A. Thomas, A. J. Millis, P. E. Sulewski, J. Orenstein, D. H. Rapkine, S-W. Cheong, and P. L. Trevor, Phys. Rev. B **42**, 10 785 (1990).
[15]S. L. Cooper, G. A. Thomas, J. Orenstein, D. H. Rapkine, A. J. Millis, S-W. Cheong, A. S. Cooper, and Z. Fisk, Phys. Rev. B **41**, 11 605 (1990).
[16]J. G. Zhang, X. X. Bi, E. McRae, P. C. Eklund, B. C. Sales, and M. Mostoller, Phys. Rev. B **43**, 5389 (1991).
[17]J.L. Brebner, S. Jandl, and Y. Lépine, Phys. Rev. B **23**, 3816 (1981); P. Rochon, J.L. Brebner, and D. Matz, Solid State Commun. **29**, 63 (1979).
[18]G. Binnig, A. Baratoff, H.E. Hoenig, and J.G. Bednorz, Phys. Rev. Lett. **45**, 1352 (1980).
[19]J.F. Schooley, W.R. Hosler, and M.L. Cohen, Phys. Rev. Lett. **12**, 474 (1964).
[20]G. A. Thomas, D. H. Rapkine, S. L. Cooper, S-W. Cheong, A. S. Cooper, L. F. Schneemeyer, and J. V. Waszczak, Phys. Rev. B **45**, 2474 (1992).
[21]G. A. Thomas, D. H. Rapkine, S. L. Cooper, S-W. Cheong, and A. S. Cooper, Phys. Rev. Lett. **67**, 2906 (1991).
[22]Y. Tokura, H. Takagi, and S. Uchida, Nature (London) **337**, 345 (1989).
[23]W. Sadowski, H. Hagemann, M. Francois, H. Bill, M. Peter, E. Walker, and K. Yvon, Physica C **170**, 103 (1991).
[24]E. T. Heyen, G. Kliche, W. Kress, W. König, M. Cardona, E. Rampf, J. Prade, U. Schröder, A. D. Kulkarni, F. W. de Wette, S. Piñol, D. McK. Paul, E. Morán, and M. A. Alario-Franco, Solid State Commun. **74**, 1299 (1990).
[25]M.K. Crawford, G. Burns, G.V. Chandrashekhar, F.H. Dacol, W.E. Farneth, E.M. McCarron III, and R.J. Smalley, Phys. Rev. B **41**, 8933 (1990).
[26]G. Burns, *Solid State Physics* (Academic, New York, 1985), pp. 467 and 468.
[27]The exceedingly high values for ϵ_∞ reported by Zhang *et al.* (Ref.16) and by Crawford *et al.* (Ref. 25) are probably due to the fact that they include in ϵ_∞ the contribution of the charge transfer band, which in our case is explicitly extracted from $R(\omega)$.
[28]G.A. Thomas, M. Capizzi, F. DeRosa, R.N. Bhatt, and T.M. Rice, Phys. Rev. B **23**, 5472 (1981).
[29]M. Reedik, D. A. Bonn, J. D. Garrett, J. A. Greedan, C. V. Stager, T. Timusk, K. Kamarás, and D. B. Tanner, Phys. Rev. B **38**, 11 981 (1988).
[30]Notice that the introduction of an oscillator at energy lower than that of the term d would allow us to neglect the Drude contribution in the x=0.04 insulating $Nd_{2-x}Ce_xCuO_4$ sample.
[31]G. Kotliar, P.A. Lee, and N. Read, Physica C **153-155**, 538 (1988).
[32]Ju.H. Kim, K. Levin, R. Wentzcovitch, and A. Auerback, Phys. Rev. B **40**, 11 378 (1989).
[33]M. Grilli, B.G. Kotliar, and A.J. Millis, Phys. Rev. B **42**, 329 (1990).
[34]M. Grilli, C. Castellani, and C. Di Castro, Phys. Rev. B **42**, 6233 (1990).
[35]P.A. Lee, G.K. Kotliar, and N. Read, Physica B **148**, 274 (1987).
[36]C.L. Kane, P.A. Lee, and N. Read, Phys. Rev. B **39**, 6880 (1989).
[37]W. Stephan and H. Horsch, Phys. Rev. B **42**, 8736 (1990).
[38]T. Tohyama and S. Maekawa, J. Phys. Soc. Jpn. **60**, 53 (1991).